IEEE Access
Multidisciplinary | Rapid Review | Open Access Journal

Received March 27, 2021, accepted April 6, 2021, date of publication April 8, 2021, date of current version April 15, 2021.

Digital Object Identifier 10.1109/ACCESS.2021.3071969

Functionally Graded Multilayered Soil Models, an Alternative to Modeling the Soil Electrical Resistivity for Computing the Grounding Resistance

R. PARAMO, E. FALEIRO, G. ASENSIO, AND J. MORENO
Departamento IEEF, Escuela Técnica Superior de Ingeniería y Diseño Industrial, Universidad Politécnica de Madrid, 28012 Madrid, Spain
Corresponding author: E. Faleiro (eduardo.faleiro@upm.es)

ABSTRACT Alternative models of the electrical resistivity of the soil to the well-known constant piecewise multilayer model are presented in this paper. By their special features, the proposed models lead to reasonably simple semi-analytical expressions for the electric potential. The parameters associated with these models are obtained from apparent resistivity measurements using an optimization procedure. The proposed models allow obtaining a continuous piecewise resistivity profile as a function of depth from the soil surface. From the full definition of the models, the grounding resistance of several electrodes is calculated and compared with that obtained from the classic multilayer model. Finally some application examples including data from field measurements are considered in this paper.

INDEX TERMS Functionally graded multilayered soil model, continuous piecewise soil resistivity, grounding resistance calculations.

I. INTRODUCTION

Determining the conductive properties of the soil is a fundamental requirement when designing a grounding system. In the theoretical calculation stage, it is necessary to choose a model for the electrical conductivity of the soil in order to calculate the grounding resistance that the chosen electrode will have [1]. From a general point of view, it would be necessary to solve the equation $\vec{\nabla} \cdot (\sigma(\vec{r})\vec{\nabla}\phi(\vec{r})) = 0$ together with some boundary conditions, where $\phi(\vec{r})$ is the absolute potential at the sourceless point $\vec{r}$ and $\sigma(\vec{r})$ is the function that represents the point conductivity of the ground. For a generic $\sigma(\vec{r})$ function, the above equation can only be approached by numerical methods, FEM, BEM and others, while for some specific models of conductivity it is possible to find acceptable semi-analytical solutions. Such is the case with the commonly used multilayer model. This model assumes that conductivity is just a function of depth z, which is a non-continuous piecewise constant function. Thus, the soil is composed of horizontal layers of infinite extension and defined thickness in which the electrical conductivity takes a constant and different value in each layer. It is quite obvious that a real soil does not generally have such a behavior, being only an approximation that will be the more accurate, the more different layers with different conductivity are considered. Thus, the actual conductivity is replaced by a step function although in practice, due to the difficulty of the calculations, only a few layers are considered [2].

The choice of a constant conductivity in each layer allows calculating the potential in the region of space occupied by each layer from a Laplace/Poisson equation arising from the equation for a generic conductivity. The connection between the solutions corresponding to each layer is made by imposing the continuity of the potential at the different interfaces $\phi_i(\vec{r}_{i,i+1}) = \phi_{i+1}(\vec{r}_{i,i+1})$ as well as the continuity of the normal component of the current density through interfaces $\sigma_i \cdot \vec{\nabla}\phi_i \cdot \vec{n}\,|_{\vec{r}_{i,i+1}} = \sigma_{i+1} \cdot \vec{\nabla}\phi_{i+1} \cdot \vec{n}\,|_{\vec{r}_{i,i+1}}$, where $\vec{n}$ stands for the normal vector to the interface shared by layers i and $i+1$.

Thanks to the cylindrical symmetry of the potential, which is associated with conductivity dependent only on the depth as the z coordinate, the common procedure to solve the equation for the potential is to use the method of separation of variables in a cylindrical coordinate system. Thus, the potential created in layer j by an electric point current source of strength I in layer i could be written as

$$\phi_{ij} = \frac{\rho_i I}{4\pi\,|\vec{r}_i - \vec{r}_j|} + \int_0^\infty (f_{ij}(\lambda)e^{-\lambda(z_i - z_j)} + g_{ij}(\lambda)e^{\lambda(z_i - z_j)}) \times J_0(\lambda r)d\lambda \quad (1)$$

The associate editor coordinating the review of this manuscript and approving it for publication was Fabrizio Messina.

where ρ_i is the constant resistivity of layer i, $r = \sqrt{(x_i - x_j)^2 + (y_i - y_j)^2}$ and J_0 is the zero-order Bessel function [3]–[5]. In (1) the functions $f_{ij}(\lambda)$ and $g_{ij}(\lambda)$ must be calculated from the boundary conditions at the interfaces above mentioned. Despite the apparent simplicity of the method, the calculation of the functions f and g can be quite difficult and the evaluation of the integral in (1) is only approximate due to the oscillatory character of the Bessel function together with the singularities of the f and g functions themselves [6].

To carry out everything described above, it is necessary to assign values to the resistivity of the considered layers. This part of the problem is of great importance since the calculations of the grounding resistance depend on the assignment of resistivity to the different layers of the model. The method used to find the multilayer resistivity profile starts from the direct measurement in the field of the apparent resistivity of the soil by means of a vertical electrical sounding (VES) with some device such as the Wenner or Schlumberger array [7]. The apparent resistivity is closely related to the soil model, and therefore to the resistivity profile of the different layers. Thus, it is in principle possible to deduce this profile from the apparent resistivity measurements [8]–[10]. This problem falls into the category of so-called inverse problems, which are very often ill-conditioned [11], [12], which means in practice that uncertainties in the measurements of apparent resistivity can produce very dramatic changes in the profile of resistivity of the multilayered model. Consequently, there is no single solution to the resistivity profile from the apparent resistivity of a soil.

In this paper, an alternative multilayered model will be presented. Although it contains many of the difficulties found in the model described above, it presents some characteristics that provide a more realistic description of the soil structure. To begin with, the electrical conductivity in the layers is no longer constant but can be adjusted to specific continuous functions in the z coordinate that will be described later. In addition, sometimes the function in each layer can be chosen so that the conductivity is globally continuous in the z coordinate. Also, the functions that represent the conductivity in each layer give rise to simple solutions for the potential, as will be seen later. The proposed model will be called Functionally Graded Multilayered Soil model (FGMS). The model is based on the seminal background that can be found in references [13], [14], which will be briefly described in the next section. The objectives of this paper are, namely, to present the FGMS model and its characteristics, to set its fundamental parameters from measurements of apparent resistivity, to establish the method for calculating potentials in the soil and finally to apply the theoretical framework to practical cases.

To achieve these objectives, the paper is organized as follows. Following the present introduction, the foundations of the FGMS method are presented in section 2. In section 3, the procedure for setting the conductivity parameters in each layer from the apparent resistivity measurements is described. The calculation of the grounding resistance of some simple electrodes in soils with synthetic FGMS models and some others coming from real apparent resistivity profiles are presented in section 4. A comparison with the results coming from equivalent conventional multilayer models is also performed in the same previous section. Finally, in section 5 the conclusions of this work are summarized..

II. FUNCTIONALLY GRADED MULTILAYER SOIL MODEL BACKGROUNDS

Let us consider a point current source of strength I located at $\vec{r}_P$ in a semi-infinite soil ($z \geq 0$) whose conductivity is a function $\sigma(\vec{r})$. The potential $\phi(\vec{r})$ generated at point $\vec{r}$, also called Green's function, is the solution of the boundary value problem (BVP)

$$\begin{aligned} &\vec{\nabla} \cdot (\sigma(\vec{r})\vec{\nabla}\phi(\vec{r})) = -I\delta(\vec{r} - \vec{r}_P) \\ &\vec{\nabla}\phi \cdot \vec{n}_z\,|_{z=0} = 0 \\ &\phi(\vec{r} \to \infty) = 0 \end{aligned} \tag{2}$$

The BVP (2) is difficult to solve in general. By the change $u = \phi \cdot \sqrt{\sigma}$, (2) becomes in the following equation for the new variable $u(\vec{r})$ [14], [15],

$$\vec{\nabla}^2 u(\vec{r}) - \frac{\vec{\nabla}^2(\sqrt{\sigma(\vec{r})})}{\sqrt{\sigma(\vec{r})}} u(\vec{r}) = -\frac{I}{\sqrt{\sigma(\vec{r})}}\delta(\vec{r} - \vec{r}_P) \tag{3}$$

When the conductivity $\sigma(\vec{r})$ only depends on the z coordinate, the second term from the left hand side of (3) becomes $\frac{1}{\sqrt{\sigma(z)}}\frac{d^2\sqrt{\sigma(z)}}{dz^2}\vec{u} = F\vec{u}$ where the operator F acting on $\vec{u}$ will be forced to take a constant value. Three interesting situations can be considered.

Case-1: The constant value F is set to zero. By solving for $\sigma(z)$, it is found that $\sigma(z) = (C_1 \cdot z + C_2)^2$ which will be called as parabolic model. In this case (3) becomes a Poisson equation in the $u(\vec{r})$ variable. The solution for a single point current source of strength I in an infinite medium is straightforward, and also for the potential $\phi(\vec{r})$,

$$\begin{aligned} \vec{\nabla}^2 u(\vec{r}) &= -\frac{I}{\sqrt{\sigma(\vec{r})}}\delta(\vec{r} - \vec{r}_P) \\ u(\vec{r}) &= \frac{I}{4\pi\sqrt{\sigma(\vec{r}_P)}\,|\vec{r} - \vec{r}_P|} \\ \phi(\vec{r}) &= \frac{I}{4\pi\sqrt{\sigma(\vec{r}_P)}\sqrt{\sigma(\vec{r})}\,|\vec{r} - \vec{r}_P|} \end{aligned} \tag{4}$$

Case-2: Next the constant value F is set to β^2, for which the conductivity is $\sigma(z) = (C_1 \cdot e^{\beta \cdot z} + C_2 \cdot e^{-\beta \cdot z})^2$, which will be called as exponential model and (3) becomes a modified Helmholtz equation [16]. The solution for $u(\vec{r})$ and $\phi(\vec{r})$ in an infinite medium is,

$$\begin{aligned} \vec{\nabla}^2 u(\vec{r}) - \beta^2 u(\vec{r}) &= -\frac{I}{\sqrt{\sigma(\vec{r})}}\delta(\vec{r} - \vec{r}_P) \\ u(\vec{r}) &= \frac{I\exp(-\beta\,|\vec{r} - \vec{r}_P|)}{4\pi\sqrt{\sigma(\vec{r}_P)}\,|\vec{r} - \vec{r}_P|} \\ \phi(\vec{r}) &= \frac{I\exp(-\beta\,|\vec{r} - \vec{r}_P|)}{4\pi\sqrt{\sigma(\vec{r}_P)}\sqrt{\sigma(\vec{r})}\,|\vec{r} - \vec{r}_P|} \end{aligned} \tag{5}$$

Case-3: Finally, if the constant value F is set to $-\beta^2$, the conductivity of the soil is found to be $\sigma(z) = (C_1 \cdot \cos(\beta \cdot z) + C_2 \cdot \sin(\beta \cdot z))^2$, which will be called as trigonometric model and (3) becomes a Helmholtz equation [17]. This time, a solution for $u(\vec{r})$ and $\phi(\vec{r})$ in an infinite medium is,

$$\begin{aligned} \vec{\nabla}^2 u(\vec{r}) + \beta^2 u(\vec{r}) &= -\frac{I}{\sqrt{\sigma(\vec{r})}}\delta(\vec{r}-\vec{r}_P) \\ u(\vec{r}) &= \frac{I\cos(\beta\,|\vec{r}-\vec{r}_P|)}{4\pi\sqrt{\sigma(\vec{r}_P)}\,|\vec{r}-\vec{r}_P|} \\ \phi(\vec{r}) &= \frac{I\cos(\beta\,|\vec{r}-\vec{r}_P|)}{4\pi\sqrt{\sigma(\vec{r}_P)}\sqrt{\sigma(\vec{r})}\,|\vec{r}-\vec{r}_P|} \end{aligned} \tag{6}$$

Note that (6) could admit complex solutions as well as real ones. Only real solutions stand for a physical potential, but the one shown in (6) is not the only possible. Due to its special features which give it great complexity, this model will not be considered initially in this work, deserving a separate study.

As already mentioned before, (4)-(6) are valid to describe the potential created by a single point current source I in an infinite medium, since no boundary condition has been imposed. When a semi-infinite medium is considered, the general solution must contain the solutions for the homogeneous equations derived from (4)-(6) to which the boundary conditions must be imposed.

For a semi-infinite medium composed by horizontal layers where a conductivity of the type described in cases 1-3 can be defined in each layer, what in this paper is called FGMS model, a cylindrical coordinates system can be used to solve the homogeneous equations associated to (4)-(6). For instance, referred to the exponential model of case 2 for a point current source located in the i layer at $\vec{r}_P$, the potential at any point $\vec{r}$ of the j layer $\phi_{ij}(\vec{r})$ can be expressed as

$$\begin{aligned} \phi_{ij}(\vec{r}) &= \frac{I\exp(-\beta\,|\vec{r}-\vec{r}_P|)}{4\pi\sqrt{\sigma_i(\vec{r}_P)}\sqrt{\sigma_j(\vec{r})}\,|\vec{r}-\vec{r}_P|}\delta_{ij} \\ &+ \int_0^\infty (f_{ij}(\lambda)e^{-\sqrt{\lambda^2+\beta_i^2}(z-z_P)} + g_{ij}(\lambda)e^{\sqrt{\lambda^2+\beta_i^2}(z-z_P)})J_0(\lambda r)d\lambda \end{aligned} \tag{7}$$

where δ_{ij} is the Kronecker delta and the unknown functions f_{ij} and g_{ij} need to be calculated by imposing the boundary conditions at each interface, namely $\vec{\nabla}\phi_{i1}\cdot\vec{n}_z\,|_{z=0} = 0$ stands for the null current flux through the soil surface and

$$\begin{aligned} &\phi_{ij}(\vec{r}_{j,j+1}) = \phi_{ij+1}(\vec{r}_{j,j+1}) \\ &\sigma_j\cdot\vec{\nabla}\phi_{ij}\cdot\vec{n}\,\Big|_{\vec{r}_{j,j+1}} = \sigma_{j+1}\cdot\vec{\nabla}\phi_{ij+1}\cdot\vec{n}\,\Big|_{\vec{r}_{j,j+1}} \end{aligned} \tag{8}$$

guarantees continuity of potential and normal current flux conservation through the interface separating the layers j and $j+1$. In (7)-(8), $\sigma_i(z) = (C_{i1}\cdot e^{\beta_i\cdot z} + C_{i2}\cdot e^{-\beta_i\cdot z})^2$ stands for the exponential model conductivity.

In order to properly implement the boundary conditions (8), it is necessary to convert the first term on the right hand of (7) to an integral form so that the entire expression is in an integral form. The integral forms of Lipschitz (9) [18], allow such a conversion to be carried out.

$$\begin{aligned} \frac{1}{|\vec{r}-\vec{r}_P|} &= \int_0^\infty e^{-\lambda\cdot|z-z_P|}J_0(r\lambda)d\lambda \\ \frac{e^{-\beta\cdot|\vec{r}-\vec{r}_P|}}{|\vec{r}-\vec{r}_P|} &= \int_0^\infty \frac{\lambda}{\sqrt{\lambda^2+\beta^2}}e^{-\sqrt{\lambda^2+\beta^2}\cdot|z-z_P|}J_0(r\lambda)d\lambda \end{aligned} \tag{9}$$

Thus, the boundary conditions (8) lead to a linear system in the unknowns f_{ij} and g_{ij} that is solved by symbolic calculus using the software Wolfram-Mathematica.

With the help of the point current source potentials (7), the potential acquired by an active electrode can be calculated using the superposition law as will be seen next. Thus, the grounding resistance as well as the step and touch potentials can be obtained. Similar expressions to (7) can be found when the other conductivity models are considered.

The expression (7) stands for the potential generated by a single point current source. When an extended electrode leaking a fault current to the ground is considered, expressions like (7) can be used under some conditions imposed to the electrodes. The electrodes are assumed as composed by thin wire pieces assembled to conform the entire electrode. Thus, each thin wire could be considered as a distribution of point current sources located in the axis. For a soil of the type defined in case 2, the potential at point $\vec{r}$ of the layer j generated by a thin wire of length L located in the layer i, is given by

$$\begin{aligned} \phi_{ij}(\vec{r}) &= \int_L \frac{\mu(\vec{r}_P)\exp(-\beta\,|\vec{r}-\vec{r}_P|)}{4\pi\sqrt{\sigma_i(\vec{r}_P)}\sqrt{\sigma_j(\vec{r})}\,|\vec{r}-\vec{r}_P|}dl_P\cdot\delta_{ij} \\ &+ \int_L \frac{\mu(\vec{r}_P)}{4\pi\sqrt{\sigma_i(\vec{r}_P)}\sqrt{\sigma_j(\vec{r})}}[\int_0^\infty (\hat{f}_{ij}(\lambda)e^{-\sqrt{\lambda^2+\beta_i^2}(z-z_P)} \\ &+ \hat{g}_{ij}(\lambda)e^{\sqrt{\lambda^2+\beta_i^2}(z-z_P)})J_0(\lambda r)d\lambda]dl_P \end{aligned} \tag{10}$$

where $\mu(\vec{r}_P)$ stands for the point current sources density along the thin wire axis and the functions $\hat{f}_{ij}$ and $\hat{g}_{ij}$ need to be calculated, again imposing the boundary conditions at each interface. In practice, the thin wire is segmented in M short pieces each of them with constant point current sources density $\{\mu_k\}_{k=1\cdots M}$, which are used to calculate the potential of the electrode itself by imposing a constant value of such potential along the entire electrode. This procedure, known as moment method, gives rise to a system of linear equations whose unknowns are the constant densities of point current sources in each segment [19], [20]. The knowledge of these densities allows the calculation of the potential at any point on the ground by superposition.

III. FITTING THE SOIL TO FGMS MODEL FROM APPARENT RESISTIVITY PROFILES

As seen in the previous section, once the FGMS model has been defined, the calculation of the potential generated by a

point current source is given by (7) if the exponential model is chosen. Expressions similar to (7) can be proposed for the other two FGMS models, parabolic and trigonometric. In this section the problem of setting the constants associated with the chosen model will be addressed. Focusing on the exponential FGMS model, from the apparent resistivity measurements using a Wenner linear quadrupole array, it is possible to find the three parameters associated with each layer of the model. Indeed, for point-like electrodes as Wenner probes separated a distance a, the measured apparent resistivity is given by

$$\rho_{app}^{meas}(a) = \frac{\Delta V(a)}{I} 2\pi a \tag{11}$$

where $\Delta V(a)$ is the potential difference between the measuring electrodes when the active electrodes are powered by a current I. From the FGMS exponential model, it is not difficult to show that

$$\rho_{app}(a; \{C_{i1}, C_{i2}, \beta_i\}) = 4\pi a(\phi_{11}(a; \{C_{i1}, C_{i2}, \beta_i\}) - \phi_{11}(2a; \{C_{i1}, C_{i2}, \beta_i\})) \tag{12}$$

where it has been enhanced that the potential depends on the parameters of the model used, in this case the exponential model. The model parameters can be found by an algorithm that minimizes

$$\chi^2 = [\rho_{app}^{meas}(a) - \rho_{app}(a; \{C_{i1}, C_{i2}, \beta_i\})]^2 \tag{13}$$

by using the Matlab routine fminsearch in a code designed for this calculation. This procedure allows obtaining the parameters that define the function that represents the electrical conductivity in each layer. Note that conductivity is non-continuous piecewise in general since no supplementary conditions have been imposed on the interfaces. The variable conductivity model proposed here in each layer is only an approximation somewhat closer to real world than the well-known multilayer model. Nevertheless, it is possible to add conditions to the parameters in the minimization process described above, to ensure that the discontinuity at the interfaces is the minimum possible. Such models will be classified as quasi-continuous models. The Lagrange multipliers method can be used to force continuity of conductivity at interfaces by expanding (13) to

$$\chi^2 = [\rho_{app}^{meas}(a) - \rho_{app}(a; \{C_{i1}, C_{i2}, \beta_i\})]^2 + \sum_i \lambda_i \cdot (\sigma_i(\{C_{i1}, C_{i2}, \beta_i\}; z) - \sigma_{i+1}(\{C_{i+11}, C_{i+12}, \beta_{i+1}\}; z))^2 \tag{14}$$

where λ_i stand for the Lagrange multipliers whose number is equal to the number of interfaces, σ_i and σ_{i+1} are the conductivities on both sides of the interface i and z takes the value of the interface depth. This will not always improve the results obtained with the associated non-continuous model, although it is obvious that if the real conductivity behaves like a continuous FGMS model, continuity will arise by itself.

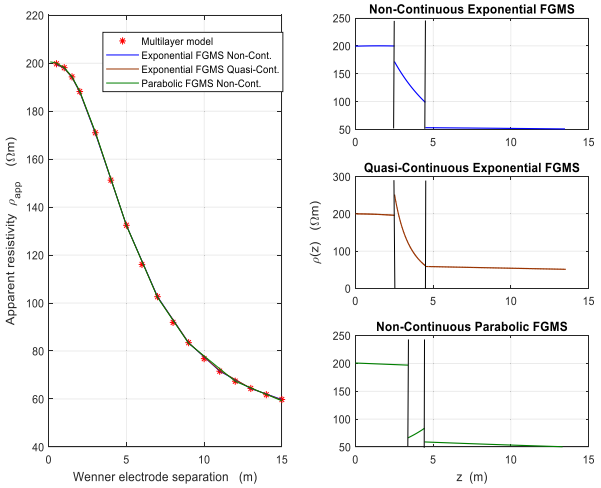

FIGURE 1. Apparent resistivity profile from a conventional three-layer model defined in the text (red stars). The subfigure shows the resistivity profile ρ(z) of different FGMS models giving rise to the apparent resistivity profile shown.

Here are some examples. Let us first consider a synthetic soil, labeled as S1, whose apparent resistivity profile is obtained from a conventional three-layer model of parameters $\rho_1 = 200$ Ωm, $\rho_2 = 100$ Ωm, $\rho_3 = 50$ Ωm, $h_1 = 3$ m, $h_2 = 3$ m.

Figure 1 shows on the left panel the apparent resistivity profile from the three-layer model (red stars) together with the calculated apparent resistivity profile from (10) when the different three-layer FGMS models that are shown in the right panel are considered. In the right panel the resistivity profile as a function of the z coordinate for a non-continuous exponential FGMS model, a quasi-continuous exponential FGMS model and a non-continuous parabolic FGMS model are shown, all of them giving rise to the apparent resistivity profile shown in the left panel

Consider next a second apparent resistivity profile, this time obtained from a real soil located at Yepes, Toledo (Spain) and labeled as S2. The measurement was carried out with a Chauvin-Arnoux model CA6472 tellurometer. The measured data corresponds to an electrode spacing ranging from 0.5 m to 15 m. The profile is shown in the left panel of Fig. 2 with green diamonds. The superimposed curves correspond to the calculated apparent resistivity by using (12) when the parameters of a conventional three-layer model and those corresponding to the listed three-layer FGMS models are used. The resistivity profiles of the FGMS models are shown in the right panel which correspond to a non-continuous exponential, quasi-continuous exponential and non-continuous parabolic model. The conventional three-layered model parameters are found to be $\rho_1 = 85.6$ Ωm, $\rho_2 = 173.2$ Ωm, $\rho_3 = 51.7$ Ωm, $h_1 = 1.8$ m, $h_2 = 2.5$ m.

Finally, Fig. 3 shows another example of apparent resistivity measured in the field in a place located at San Sebastián de los Reyes, Madrid (Spain) and labeled as S3. The device used for measurement was a Geohm-c (Gossen Metrawatt) tellurometer. Here, the measured data also corresponds to an

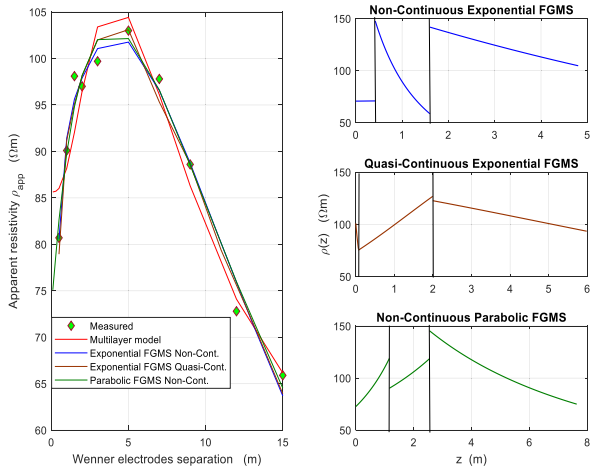

FIGURE 2. Apparent resistivity profile (green diamonds) from a Wenner sounding located at Yepes, Toledo (Spain). The right panel shows the three-layered FGMS models for ρ(z) of the soil obtained from such an apparent resistivity profile by (13) and (14).

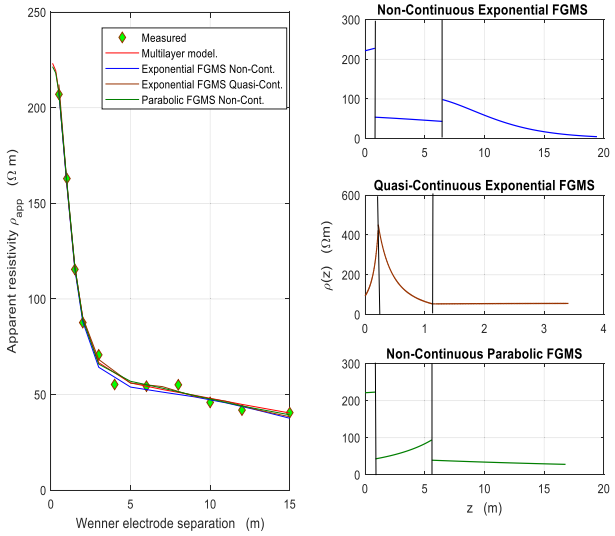

FIGURE 3. Apparent resistivity profile from a Wenner sounding located at San Sebastián de los Reyes, Madrid (Spain). The right panel shows the three-layered FGMS models for ρ(z) of the soil obtained from such an apparent resistivity profile by (13) and (14).

electrode spacing ranging from 0.5 m to 15 m. As in the previous example, the left panel shows the measured apparent resistivity profile (green diamonds) together with those calculated by using (10) from the conventional three-layer model with parameters $\rho_1 = 223.4\ \Omega$m, $\rho_2 = 54.3\ \Omega$m, $\rho_3 = 19.0\ \Omega$m, $h_1 = 0.8$ m, $h_2 = 1.2$ m, and the parameters of a non-continuous exponential, quasi-continuous exponential and non-continuous parabolic model whose resistivity profiles are shown in the right panel. Although the first layer in the quasi-continuous model shows increasing resistivity with depth, the measured apparent resistivity decreases because the first spacing considered is 0.5m while the width of the layer is only 0.22 m.

Table 1 and Table 2 summarize the parameter values for the exponential FGMS models used. In both tables, soils are

TABLE 1. Non-continuous FGMS exponential model parameters for soils s1 to s3.

	S1	S2	S3
C_{11}	0.0358	0.1591	0.1608
C_{12}	0.0349	-0.0402	-0.0936
β_1	0.0515	-0.0020	-0.0045
C_{21}	0.0861	0.1836	0.0864
C_{22}	-0.0976	-0.1180	0.0481
β_2	0.1590	0.1308	0.0453
C_{31}	0.0995	0.0707	0.0242
C_{32}	0.0269	0.0074	0.0973
β_3	0.0119	0.0549	0.1500
h_1	2.52	0.42	0.82
h_2	1.99	1.18	5.66

TABLE 2. Quasi-continuous FGMS exponential model parameters for soils s1 to s3.

	S1	S2	S3
C_{11}	0.0358	0.3448	-0.3017
C_{12}	0.0349	-0.2453	0.4051
β_1	0.0515	0.3711	0.3537
C_{21}	0.0861	0.1015	0.2193
C_{22}	-0.0976	0.0150	-0.1934
β_2	0.1590	-0.2193	0.2320
C_{31}	0.0995	0.0576	0.0892
C_{32}	0.0269	0.0283	0.0499
β_3	0.0119	0.0631	-0.0753
h_1	2.52	0.07	0.22
h_2	1.95	1.93	0.92

labeled S1 for synthetic soil, S2 for soil located at Yepes, and S3 for soil located at San Sebastian de los Reyes. The parameters in Table 1 correspond to the unconstrained minimization process giving rise to non-continuous FGMS exponential models. The SI units of parameter C_{i1} are $(\Omega m)^1/2$ while those of C_{i2} are $(\Omega m)^1/2$ and m^{-1} for β_k. When the continuity at the interfaces is introduced by means of Lagrange multipliers, other values for the parameters are obtained which are collected in Table 2.

Table 3 shows the parameter values for the FGMS parabolic model of the same soils S1 to S3. No conditions are imposed at the interfaces, thus the conductivity results non-continuous piecewise. The SI units of parameter C_{i1} are $(\Omega/m)^1/2$ while those of C_{i2} are $(\Omega m)^1/2$.

Finally, Table 4 shows the parameter values of a conventional multilayer model for the considered soils. Regarding the parameters of Table 4, the SI units are the usual ones, this is Ωm for ρ_i and m for h_j.

IV. MODEL TEST: GROUNDING RESISTANCE AS A FUNCTION OF THE BURIAL DEPTH

In this section, the grounding resistance of several simple electrodes will be calculated as a function of the burial depth. In addition to the conventional multilayer model,

TABLE 3. Non-continuous FGMS parabolic model parameters for soils s1 to s3.

	S1	S2	S3
C_{11}	0.0001	-0.0221	-0.0003
C_{12}	0.0706	0.1173	0.0672
C_{21}	-0.0002	-0.0097	-0.0105
C_{22}	0.0727	0.1165	0.1618
C_{31}	0.0011	0.0064	0.0026
C_{32}	0.1256	0.0666	0.1450
h_1	1.70	1.16	0.88
h_2	1.88	1.39	4.72

TABLE 4. Multilayer model parameters for soils s1 to s3.

	S1	S2	S3
ρ_1	200	85.6	223.4
ρ_2	100	173.2	54.3
ρ_3	50	51.7	18.9
h_1	3	1.8	0.8
h_2	2	2.4	11.2

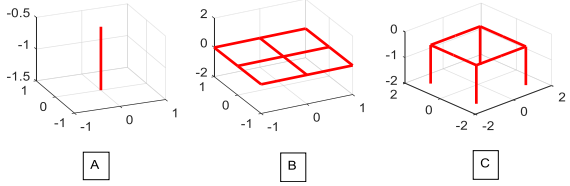

FIGURE 4. The electrodes used for testing the FGMS models.

the exponential FGMS model and the parabolic FGMS model will be considered. The soils that will be used are those used in the previous section to discuss the procedure to find the parameters of the soil models from the apparent resistivity measurement. It is a synthetic soil previously labeled as S1 and two soils measured in the field S2 and S3, whose conductivity parameters are shown in Table 1 to Table 3. Three types of electrodes will be used: a unit length vertical rod, a horizontal grid and a squared horizontal frame with vertical rods from the corners (Fig. 4).

The electrode labeled A of Fig. 4 is a vertical rod of unit length and radius r = 0.008m. Burial depth is measured from the soil surface to the top of the rod and ranges from $d = 0.01$ m to $d = 5$ m. The electrode B of Fig. 4 used for the test is a regular horizontal square grid with a 2 m edge and composed of straight conductors with a radius of 0.008 m. Just like before, burial depth is measured from the ground surface to the grid plane and again ranges from $d = 0.01$ m to $d = 5$ m. Finally, the electrode C of Fig. 4 combining horizontal and vertical conductors is considered. It is a horizontal square frame of 2.6 m on a side made of rectilinear conductors with a radius of 0.008 m, in whose corners vertical conductive rods of the same radius and 1.5 m in length are placed. The burial depth is measured from the soil surface to the frame plane and also ranges from $d = 0.01$ m to $d = 5$ m.

Those electrodes are buried into the soils S1 to S3 and the theoretical grounding resistance for the three soil models, constant multilayered model, non-continuous exponential FGMS model and non-continuous parabolic FGMS model is calculated as a function of the burial depth.

Figure 5 summarizes the results in a matrix form. Each row refers to a soil type, from S1 in the top row to S3 in the bottom row. The columns show the grounding resistance profile for each soil associated to the same test electrode. In each element of the matrix, the three mentioned models are used to find the grounding resistance profile of the electrode as a function of the burial depth.

For soils S1 and S3, a great accordance in the grounding resistance profiles is found. Figures (a) to (c) in the top row and Figures (g) to (i) in the bottom row, shows very close profiles. However, there are significant differences in grounding resistance values for some depths.

The aforementioned similarity in the grounding resistance profiles is closely related to the almost total agreement in the apparent resistivity profiles of Fig. 1 and Fig. 3. Thus, the different soil models used give rise to calculated values of grounding resistance that are not very different between them.

On the other hand, for the S2 soil, there are clear differences in the apparent resistivity profiles obtained from the different models. Observing the resistivity values in each layer provided by the different models, it is seen that the FGMS models somewhat smooth out the large oscillation that the conventional multilayer model presents. Therefore, it is expected that the grounding resistance profiles show significant differences between the different models. Figures (d) to (f) show such a different profiles. Regarding the validity of the different models, it can be said that all the models compatible with an apparent resistivity profile are valid. The grounding resistance calculated with the different models represents an approximation to the real resistance, which could only be found from the exact knowledge of the true resistivity profile of the ground.

Thus, there is an intrinsic uncertainty in the theoretical calculation of the grounding resistance of an electrode. The inability to find a single model soil model that gives rise to the measured apparent resistivity profile is at the origin of such uncertainty. Therefore, being able to have models other than the commonly used multilayered model is very useful in order to have a measure of the uncertainty in the theoretical calculation of grounding resistance.

Next we will discuss the differences between using an interface-continuous and non-continuous FGMS models of the same soil. The soil S2 is used for testing several exponential FGMS models whose parameters are shown in Table 5. The model labeled as NC corresponds to the non-continuous piecewise FGMS model (NC) and the rest correspond to quasi-continuous models QC1 (Quasi-Continuous 1) and QC2 (Quasi-Continuous 2) whose resistivity profiles are shown in Fig. 6.

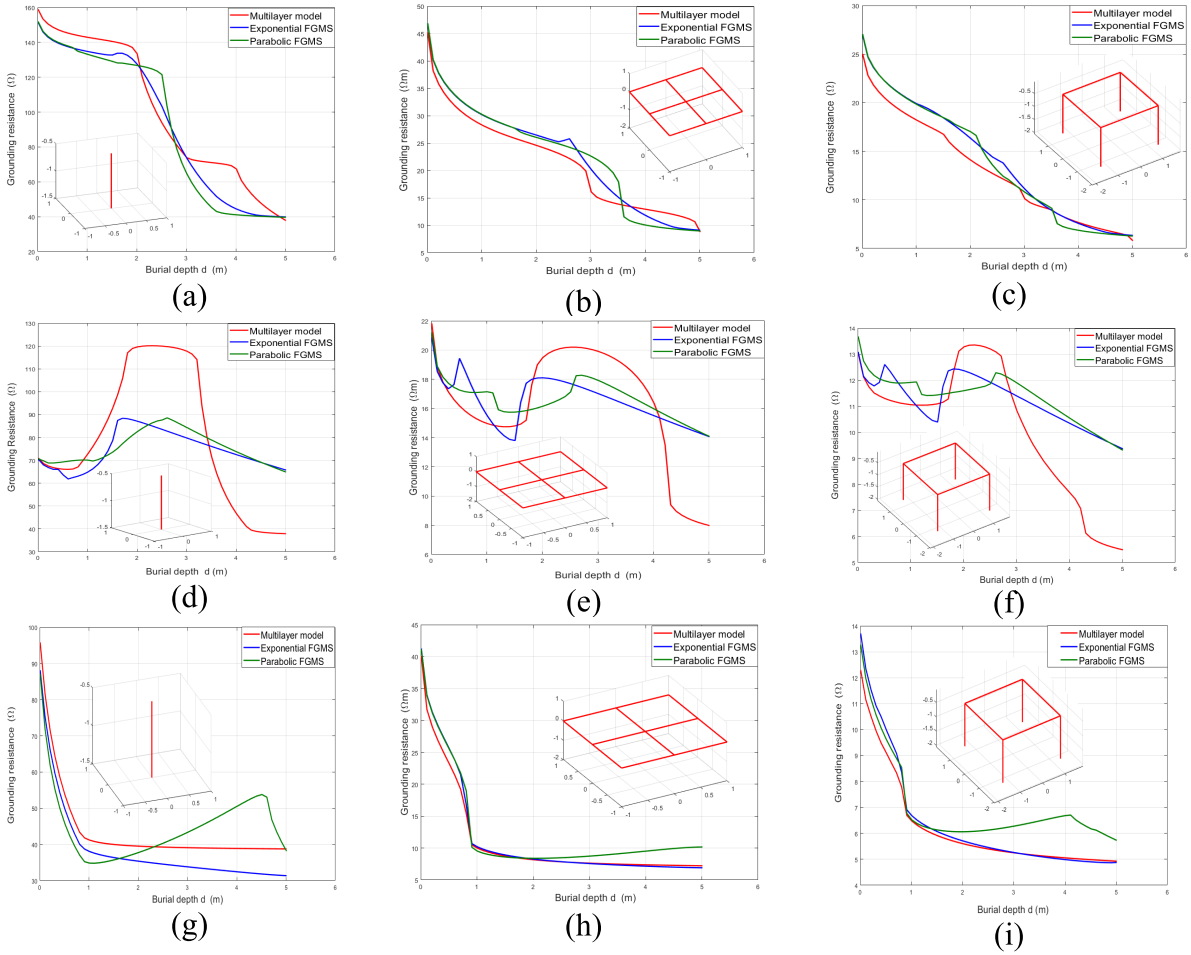

FIGURE 5. Grounding resistance as a function of the burial depth for the electrodes A to C of Fig. 4, when are buried into the soils S1 (top row), S2 (middle row) and S3 (bottom row). For each type of soil, three models have been considered, the conventional multilayer soil, the exponential FGMS model and the parabolic FGMS model.

TABLE 5. FGMS Exponential model parameters for the soil s2.

	NC	QC1	QC2
C_{11}	0.1591	0.3448	0.1855
C_{12}	-0.0402	-0.2453	-0.0948
β_1	-0.0020	0.3711	0.2442
C_{21}	0.1836	0.1015	0.2495
C_{22}	-0.1180	0.0150	-0.1172
β_2	0.1308	-0.2193	-0.0850
C_{31}	0.0707	0.0576	0.1420
C_{32}	0.0074	0.0283	-0.0641
β_3	0.0549	0.0631	0.0231
h_1	0.42	0.07	0.42
h_2	1.18	1.93	1.20

Figure 6 also shows the apparent resistivity profile for all the considered models as well as the grounding resistance versus the burial depth using the electrode C as a probe. As it can be appreciate, neat differences arise between the models in the grounding resistance profile.

In some sense, the classic multilayer model is a closed model meaning that once the apparent resistivity data is given, the constant and different values of the resistivity in each layer could be calculated. Small differences in the apparent resistivity data can give rise to very different values in the resistivity and thickness of the layers, but no continuity between adjacent layers can be obtained. Thus, a resistivity non-continuous piecewise step-type is obtained. In contrast, the FGMS models allow exploring the possibility of obtaining a continuous piecewise model by imposing the continuity of resistivity at the interfaces. In each layer, the resistivity is a function of the depth that could correspond to the true resistivity or not at all, but it is a candidate for resistivity with the same validity as the classic constant multilayer model.

A final test in the field on the S2 soil is performed. A conductive rod of 19 cm length and 8 mm radius is vertically buried and the grounding resistance is measured by the potential fall-off method using the Chauvin Arnaud P01126506 tellurometer. A grounding resistance of 212 Ω is measured. When using the constant multilayer model for the soil S2, a calculated grounding resistance of 256 Ω is obtained. However, using the Non-continuous exponential FGMS model, results a calculated resistance of 211 Ω. For the

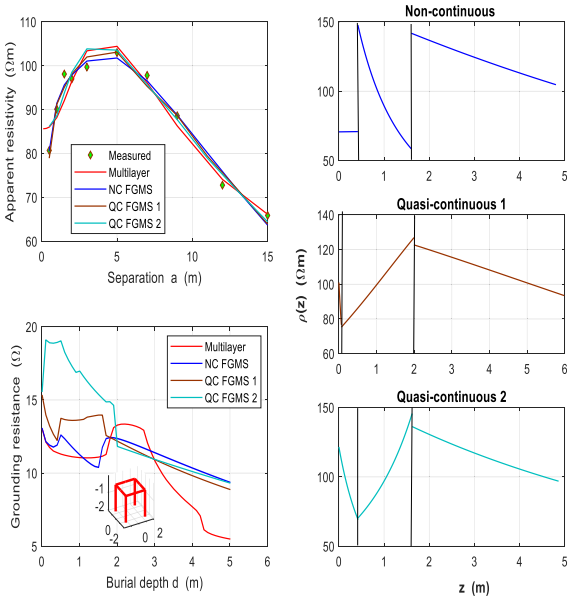

FIGURE 6. Apparent resistivity profile, grounding resistance profile and the exponential FGMS resistivity profile $\rho(z)$ of the soil S2 for three different but equivalent FGMS models.

two other FGMS models the calculated grounding resistance is 235 Ω for QC1model and 291 Ω for QC2 model.

Finally, another conductive rod of 20 cm length and 6 mm radius is also buried in other site of the previous S2 ground and the grounding resistance is again measured obtaining a value 221 Ω. The four theoretical models give rise to the calculated resistance, 267 Ω for the multilayer model, 235 Ω for the NC exponential FGMS model, 262 Ω for the QC1 model and 324 Ω for the QC2 model. Again, the exponential NC exponential FGMS model is the one that gives the best results for the calculated ground resistance.

V. CONCLUSION

Starting from an apparent resistivity profile, it is not possible to propose a unique model that defines resistivity as a function of depth. Among the resistivity models for which the calculation of the potential is relatively simple there are the classic multilayer model and the FGMS models introduced in this paper. The common characteristic of all of them is to define resistivity as a piecewise function. In the multilayer model, a constant non-continuous piecewise resistivity is found while a variable non-continuous piecewise function is on the basis of the FGMS models. A very interesting feature of FGMS models is the possibility of imposing continuity on the interfaces to obtain a continuous piecewise function. It will not always be possible to obtain strict continuity, but this expands the number of possible models of a given soil.

Among the soils studied in this paper, the synthetic soil S1 is the one that shows the greatest agreement in the grounding resistance profiles for the different models used. One of the possible explanations for this fact is the extreme regularity in the apparent resistivity profile as a result of the synthetic character of the soil. On the other hand, the real soil S2 is the one that presents the lowest agreement between the apparent resistivity curves of the different models tested since very significant differences in the non-continuous piecewise function that represents the resistivity are found and therefore appreciable differences in the grounding resistance profiles are expected.

Numerical experiments and measurements made in the field suggest that the true value of grounding resistance of an electrode belongs to an interval in which the calculated grounding resistance values from the available models of the soil are included. Soils with a smooth and accurately measured apparent resistivity profile are the ones that will provide a calculated resistance closest to the actual resistance of electrodes regardless of the model adopted for soil resistivity.

Finally, it must be added that although only three-layer FGMS models have been considered here, many soils that would only admit classic multilayer models with three or more layers could be modeled with two-layer FGMS models, thus reducing the number of parameters and simplifying somewhat later calculations.

ACKNOWLEDGMENT

The authors would like to thank the Department of Electrical Engineering, Applied Mathematics and Applied Physics of the Escuela Técnica Superior de Ingeniería *y* Diseño Industrial (ETSIDI), at Universidad Politécnica de Madrid (UPM) for their support to the undertaking of the research summarized here. Furthermore, the authors appreciate the collaboration with the firm INGESCO Lightning Solutions at Terrassa, Barcelona, Spain, for the technical support and useful suggestions for this work.

REFERENCES

[1] V. P. Androvitsaneas, K. D. Damianaki, C. A. Christodoulou, and I. F. Gonos, "Effect of soil resistivity measurement on the safe design of grounding systems," *Energies*, vol. 13, no. 12, p. 3170, 2020.

[2] E. D. Sunde, *Earth Conduction Effects in Transmission Systems*. New York, NY, USA: Dover, 1949.

[3] J. Zou, R. Zeng, J. L. He, J. Guo, Y. Q. Gao, and S. M. Chen, "Numerical Green's function of a point current source in horizontal multilayer soils by utilizing the vector matrix pencil technique," *IEEE Trans. Magn.*, vol. 40, no. 2, pp. 730–733, Mar. 2004.

[4] T. Islam, Z. Chik, M. M. Mustafa, and H. Sanusi, "Estimation of soil electrical properties in a multilayer earth model with boundary element formulation," *Math. Problems Eng.*, vol. 2012, pp. 1–13, Aug. 2012.

[5] T. Takahashi and T. Kawase, "Analysis of apparent resistivity in a multilayer earth structure," *IEEE Trans. Power Del.*, vol. 5, no. 2, pp. 608–614, Apr. 1990.

[6] K. A. Michalski and J. R. Mosig, "Efficient computation of Sommerfeld integral tails–methods and algorithms," *J. Electromagn. Waves Appl.*, vol. 30, no. 3, pp. 281–317, Feb. 2016.

[7] F. Wenner, "A method of measuring earth resistivity," Sci. Paper, Nat. Bureau Standards, Gaithersburg, MD, USA, Tech. Rep. 258, May 1916, vol. 12, no. 4, pp. 469–482.

[8] A. A. R. Zohdy, "A new method for the automatic interpretation of Schlumberger and Wenner sounding curves," *Geophysics*, vol. 54, no. 2, pp. 245–253, Feb. 1989.

[9] H. Yang, J. Yuan, and W. Zong, "Determination of three-layer earth model from Wenner four-probe test data," *IEEE Trans. Magn.*, vol. 37, no. 5, pp. 3684–3687, Sep. 2001.

[10] P. K. Gupta, S. Niwas, and V. K. Gaur, "Straightforward inversion of vertical electrical sounding data," *Geophysics*, vol. 62, no. 3, pp. 775–785, May 1997.

[11] S. Sharma and G. K. Verma, "Inversion of electrical resistivity data: A review," *Int. J. Comput. Syst. Eng.*, vol. 9, no. 4, pp. 400–406, 2015.
[12] A. I. Olayinka and U. Yaramanci, "Assessment of the reliability of 2D inversion of apparent resistivity data," *Gephysical Prospecting*, vol. 48, no. 2, pp. 293–316, 2000.
[13] A. Sutradhar and G. H. Paulino, "The simple boundary element method for transient heat conduction in functionally graded materials," *Comput. Methods Appl. Mech. Eng.*, vol. 193, nos. 42–44, pp. 4511–4539, Oct. 2004.
[14] A. Sutradhar and G. H. Paulino, "A simple boundary element method for problems of potential in non-homogeneous media," *Int. J. Numer. Methods Eng.*, vol. 60, no. 13, pp. 2203–2230, Aug. 2004.
[15] H.-Y. Kuo and T. Chen, "Steady and transient Green's functions for anisotropic conduction in an exponentially graded solid," *Int. J. Solids Struct.*, vol. 42, nos. 3–4, pp. 1111–1128, Feb. 2005.
[16] M. Tsuchimoto, K. Miya, T. Honma, and H. Igarashi, "Fundamental solutions of the axisymmetric Helmholtz-type equations," *Appl. Math. Model.*, vol. 14, no. 11, pp. 605–611, Nov. 1990.
[17] M. Tezer-Sezgin and S. Dost, "On the fundamental solutions of the axisymmetric Helmholtz-type equations," *Appl. Math. Model.*, vol. 17, no. 1, pp. 47–51, Jan. 1993.
[18] M. Abramowitz and I. A. Stegun, *Handbook of Mathematical Functions*. New York, NY, USA: Dover, 1972.
[19] R. F. Harrington, *Field Computation by Moment Methods*. New York, NY, USA: IEEE Press, 1993.
[20] W. C. Gibson, *The Method of Moments in Electromagnetics*. London, U.K.: Chapman & Hall, 2008.

R. PARAMO received the M.Sc. degree in electromechanical engineering from the Universidad Politécnica de Madrid (UPM), in 2012, where he is currently pursuing the Ph.D. degree with the IEEF Department. Since 2005, he has been an Electrical Project Manager with the firm SGS. His research interest includes grounding systems design and calculations.

E. FALEIRO received the B.S. and Ph.D. degrees in theoretical physics from the Universidad Complutense de Madrid (UCM), in 1982 and 1998, respectively. Since 1994, he has been a Full Professor with the IEEF Department, Escuela Técnica Superior de Ingeniería *y* Diseño Industrial (ETSIDI), Universidad Politécnica de Madrid (UPM).

G. ASENSIO received the B.S. degree in theoretical physics from the Universidad Complutense of Madrid (UCM), in 1987, and the Ph.D. degree in applied mathematics from the Polytechnic University of Madrid (UPM), in 2002. Since 2003, he has been a Full Professor with the Applied Mathematics Department, Escuela Técnica Superior de Ingeniería *y* Diseño Industrial (ETSIDI), UPM.

J. MORENO received the B.S. and Ph.D. degrees in industrial engineering from the Polytechnic University of Madrid (UPM), in 1989 and 1995, respectively. Since 1995, he has been a Full Professor with the Electrical Engineering Department, Escuela Tecnica Superior de Ingeniería y Diseño Industrial (ETSIDI), UPM. Since 1995, he has been the Director of the Magnetics Measurements Laboratory, UPM. He is an Expert Referee of projects for the Accreditation Agency for Research, Development and Technological Innovation (AIDIT).